SUPPLEMENTARY MATERIAL

FOR

Active rheology of membrane actin: sliding vs. sticking conditions

Silvia Isanta[a], Gabriel Espinosa[b], Ruddi Rodríguez-García[a], Paolo Natale[c], Ivan López-Montero[a], Dominique Langevin[b] and Francisco Monroy*[a]

Lipid monolayers: surface pressure and compression elasticity

As reference states, let's consider the compression isotherms of the Langmuir monolayers representative of the two binding scenarios described in the main text. Figure S1(left) shows the compression isotherms of POPC monolayers mixed with the charged lipid DODA and with the covalent linker Lip-NHS as well. In the first case, we observe an expanded isotherm typical for a disordered lipid phase.

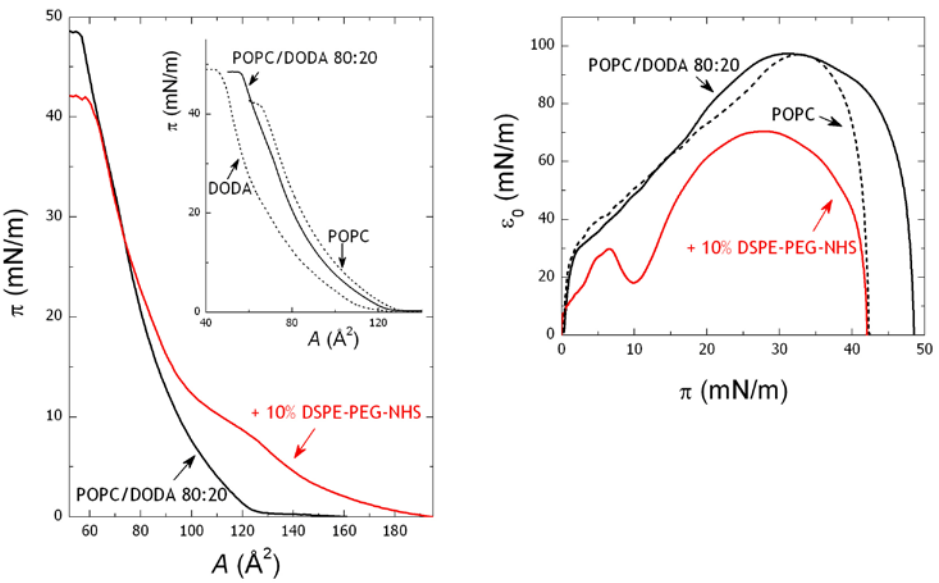

Fig. S1. Left) π–*A* compression isotherms of the lipid monolayers considered in this study (black line: 22ºC; compression rate 0.03 min^{-1}). **Right)** Compression modulus ε_0 calculated as the numerical derivative of the π–*A* curve (red line).

This isotherm is intermediate between that of the mono-unsaturated zwiterionic phospholipid (POPC) and of the fully saturated cationic surfactant (DODA) (see inset). Collapse occurs at an average molecular area *ca.* 55 $Å^2$, intermediate between the two lipids, and at a pressure *ca.* 48mN/m, higher

than POPC (≈ 42mN/m), but equal to DODA. This behavior points out the importance of coulombic interactions between charged lipids at high packing. The inclusion of Lip-NHS causes significant monolayer expansion (see Fig S1). In this case, a transition plateau is clearly observed at an intermediate pressure ($\pi_p \approx$ 10mN/m), closely coinciding with the packing transition of the PEG polymer-cores[1,2,3]. Then, an expanded-like state is re-entered at average areas lower than 100Å^2. Here, the PEG-tails accommodates brush-like in the water subphase. Finally, the monolayer collapses at the lipid close packing ($\pi \approx$ 42mN/m, $A \approx$ 55 Å^2).

Figure S1 (right) plots the compression modulus, calculated by numerical derivation of the surface pressures given in Fig. S1, $\varepsilon_0 = -(1/A)(d\pi/dA)_T$. At the relevant bilayer packing ($\pi \approx$ 30mN/m)[4,5], the POPC/DODA layer is characterized by a relatively high compression modulus, $\varepsilon_0 \approx$ 100mN/m. These experimental values are quantitatively similar to those found for other fluid lipid monolayers[6]. Inclusion of Lip-NHS causes significant softening, detected as a decrease of ε_0. In this case, two regimes exist at both sides of the transition plateau (see Fig. S1): *a)* at low pressure ($\pi \leq$ 10mN/m, $\varepsilon_0 \leq$ 30mN/m) a soft polymer-like regime characterized by the entropic elasticity of the polymer moiety[7,8]; *b)* at high pressure ($\pi >$ 10mN/m) a rigid regime dominated by the high packing of lipids. However, because of structural disordered induced by PEG, these rigid states are relatively soft with respect to the pure lipid[1-3].

F-actin unspecific adsorption: air/buffer interface and POPC monolayers

To get insight about protein binding the surface pressure was measured after protein injection in the subphase. In a typical experiment, a concentrated solution of G-actin (c_P = 10mg/ml) is injected in the Langmuir trough containing a polymerising (F-) buffer and the pressure recorded until equilibration. At the bare air/buffer interface (without lipids; Fig S2), the adsorption process follows a two-step kinetics characterised by a fast adsorption step completed after 5-10 minutes as a pseudo-plateau (at $\pi_p^{(0)} \approx$ 10mN/m) followed by a slower increase up to a final saturation value (*ca*. 18 mN/m). After 90 mins, the surface pressure does not increase anymore (it changes less than ±0.1 mN/m in one an hour), thus suggesting that the protein is fully denaturized in a state characterised by a spreading pressure, $\pi_{spr} \approx$ 18mN/m. This surface adsorption-denaturation process has been previously described under similar conditions by Renault *et al.*[9] and Demé *et al.*[10]. These authors have identified the intermediate plateau observed at $\pi_p \approx$ 10mN/m as the characteristic adsorption state of F-actin polymerised *in-situ*[9,10], which denaturates if exposed to air, as pointed out by rheological measurements[9].

When adsorption occurs under a lipid monolayer, the kinetic curves are characterised by only one adsorption step, suggesting no protein denaturalization. This is in agreement with previous studies[9,10,11]. The composite lipid/protein film is characterised by a higher pressure than the bare lipid bilayer, the pressure increase corresponding to the spontaneous adsorption of actin ($\Delta\pi = \pi_p - \pi_l$).

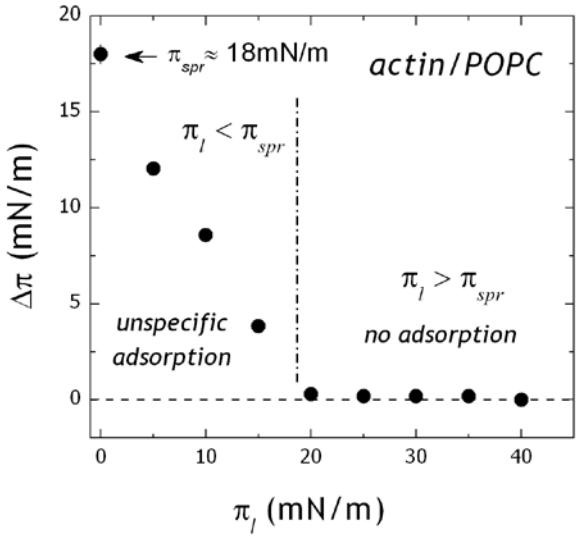

Figure S2. Increase in surface pressure ($\Delta\pi$) upon F-actin adsorption on a POPC monolayer with an initial pressure π_l. The numerical value $\Delta\pi$ can be interpreted as a surface energy gained upon protein adsorption. Unspecific protein adsorption ($\Delta\pi > 0$) only occurs at surface pressures lower than the spreading pressure of actin ($\pi_l < \pi_{spr} \approx 18$mN/m, vertical dashes). No protein adsorption is detected at higher lipid packing ($\Delta\pi \approx 0$ at $\pi_l > \pi_{spr}$).

Figure S2 shows these $\Delta\pi$–data measured after injection of 50µL actin in the subphase (at a final protein concentration, c_P = 1.4µg/mL) at different states characterised by constant π_l (the initial pressure of the pre-existing lipid monolayer). Similar results were previously published by Demé *et al*[10] for a homologous system (DMPC/actin). Likewise, the spreading pressure of F-actin (π_{spr} = 18mN/m) defines two pressure regimes: 1) $\pi < \pi_{spr}$: here F-actin co-adsorbs with the lipid causing an additional decrease in surface energy, and the pressure increase progressively lowers as the spreading pressure is approached. 2) $\pi > \pi_{spr}$: here, because the initial pressure of the lipid monolayer exceeds the spreading pressure of the protein there is no energetic reason for protein adsorption thus no pressure increase is detected ($\Delta\pi \approx 0$). The protein spreading pressure defines the transition between the two

regimes; specific binding effects will be only resolvable at a lipid packing well above π_{spr} whilst unspecific effects will dominate below.

F-actin electrostatic / covalent binding to lipid monolayers

Protein injection experiments were performed under lipid monolayers able to specifically bind F-actin (with DODA and functional Lip-NHS). The two strategies (electrostatic and covalent) were separately checked. In the two cases, positive pressure increases are systematically observed thus indicating spontaneous adsorption of protein. The results are plot in Figure S3. Again, two distinct regimes are clearly discernable, but, a binding regime characterised by a significant pressure increase is now detected at pressures above 20mN/m.

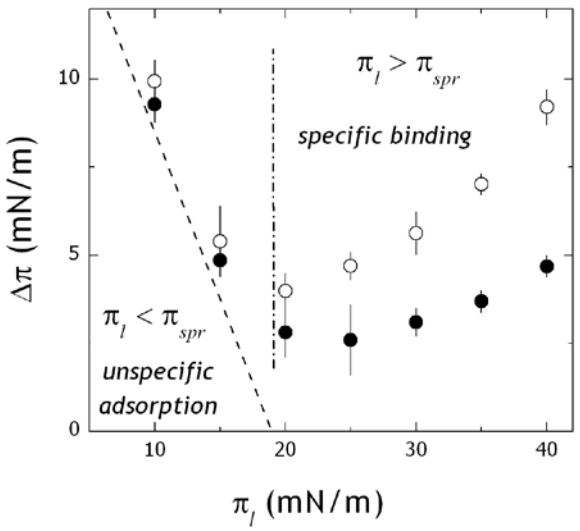

Figure S3. Adsorption pressures ($\Delta\pi$) of F-actin on lipid monolayers: (●) 80% POPC + 20% DODA (electrostatic scenario); (○) 70% POPC + 20% DODA + 10% Lip-NHS (electrostatic + covalent scenario). Again, as in Fig.4, the protein spreading pressure ($\pi_{spr} \approx$ 18mN/m, vertical dashes) determines two adsorption regimes: $\pi_l < \pi_{spr}$) unspecific adsorption; $\pi_l > \pi_{spr}$) specific binding (see text for details).

At low pressures ($\pi < \pi_{spr} \approx$ 18mN/m), the surface density of protein anchors is not high enough, thus F-actin adsorbs in a similar way than at POPC monolayers. In the high pressure regime ($\pi > \pi_{spr}$), the change in surface pressure increases again, even upon increasing lipid packing. In this regime, cationic

lipids enhance surface stability by specific binding of oppositely charged actin. Meaningfully, specific protein binding through of covalent linkers (Lip-NHS) provides complementary surface stability.

Compression viscoelasticity

We present here the whole set of experimental data obtained in compression rheology experiments performed at different packing states. The main text just focuses on the results at the bilayer- relevant packing (π = 30 mN/m), however we report all data as supplementary material (see main text for a detailed discussion)

Electrostatic binding: sliding conditions

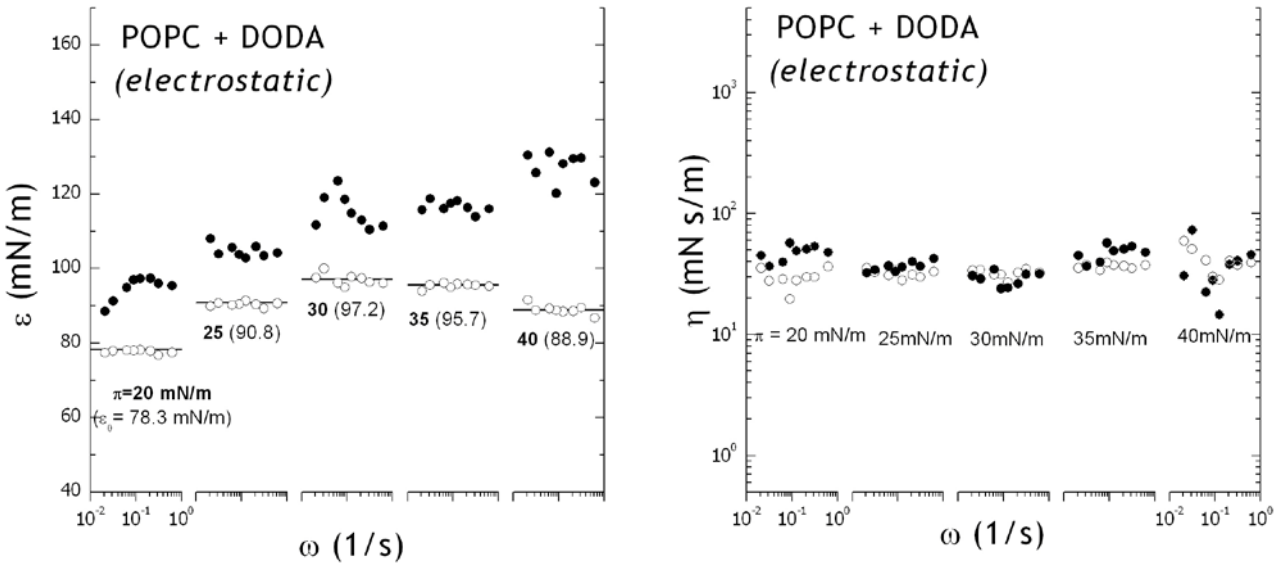

Figure S4. Left) Dynamic elasticity modulus, $\varepsilon(\omega)$, measured as a function of the deformation frequency (ω) in oscillatory barrier experiments performed on POPC + DODA (80:20) monolayers: (○) in the absence of F-actin; (●) in the presence of F-actin (5μg/mL). Different series correspond to different surface pressures of the bare lipid monolayer (π; values expressed in bold numbers). The horizontal straight lines correspond to the equilibrium compression modulus measured at every surface state (ε_0; values expressed as numbers between parentheses). **Right)** Dynamic compression viscosity, $\eta(\omega)$ (symbols as in the left figure).

Covalent anchoring: sticking conditions

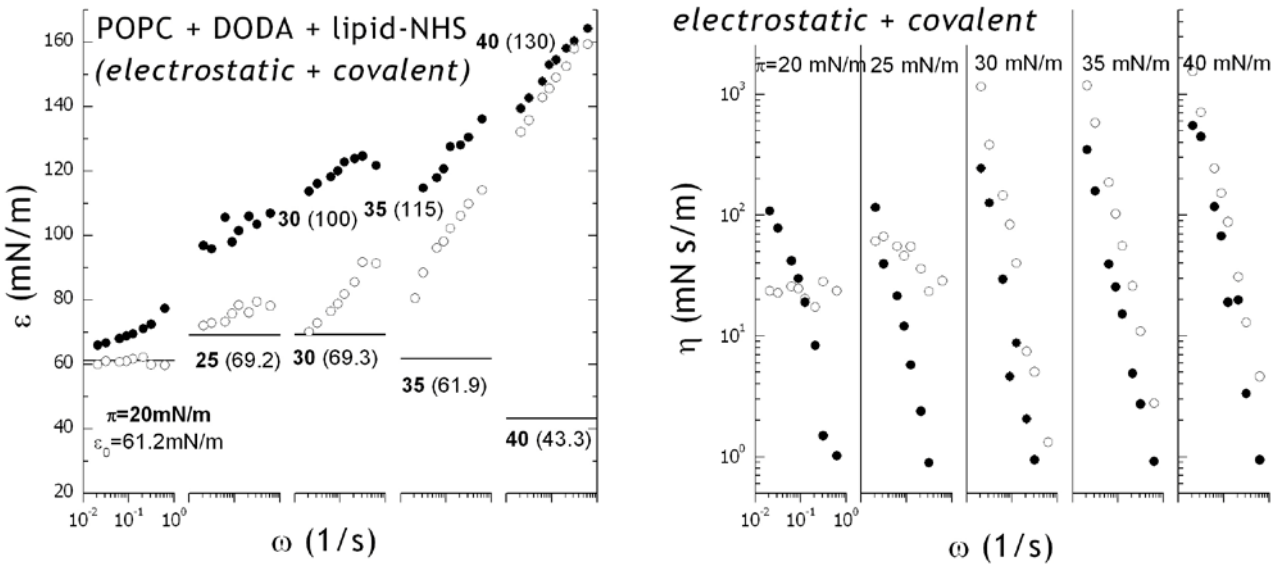

Figure S5. Left) Dynamic elasticity modulus, $\varepsilon(\omega)$, measured as a function of the deformation frequency (ω) in oscillatory barrier experiments performed on POPC + DODA + Lip-NHS (70:20:10) monolayers: (○) in the absence of F-actin; (●) in the presence of F-actin (5μg/mL). Different series correspond to different surface pressures of the bare lipid monolayer (π; values expressed in bold numbers). The horizontal straight lines correspond to the equilibrium compression modulus measured at every surface state (ε_0; values expressed as numbers between parentheses). **Right)** Dynamic compression viscosity, $\eta(\omega)$ (symbols as in the left figure).

REFERENCES

[1] V. Tsukanova and C. Salesse, *Macromolecules*, 2003, **36**, 7227.

[2] C. Naumann, C. Brooks, G. Fuller, W. Knoll and C. Frank, *Langmuir*, 1999, **15**, 7752.

[3] C. Naumann, C. Brooks, W. Wiyatno, W. Knoll, G. Fuller and C. Frank, *Macromolecules*, 2001, **34**, 3024.

[4] D. Marsh, *Biochim Biophys Acta*, 1996, **1286**, 183.

[5] M. Fidorra, A. Garcia, J. Ipsen, S. Hartel and L.A. Bagatolli, *Biochim. Biophys. Acta: Biomemb.*, 2009, **1788**, 2142.

[6] I. López-Montero, L.R. Arriaga, F. Monroy, G. Rivas, P. Tarazona and M. Vélez, *Langmuir*, 2008, **24**, 4065.

[7] F. Monroy, F. Ortega, R.G. Rubio, *Phys. Rev. E*, 1998, **58**, 629.

[8] D. Langevin and F. Monroy, *Curr. Opinion Colloid Interf. Sci*. 2010, **15**, 283.

[9] A. Renault, P. Lenne, C. Zakri, A. Aradian, C. Vénien-Bryan and F. Amblard, *Biophys. J.*, 1999, **76**, 1580-1590.

[10] B. Demé, D. Hess, M. Tristl, L. Lee and E. Sackmann, *Eur. Phys. J. E*, 2000, **2**, 125.

[11] O. Müller, H.E. Gaub, M. Bärmann, E. Sackmann, E. *Macromelecules*, 1991, **24**, 3111.